International Core Journal of Engineering Volume 11 Issue 4, 2025
ISSN: 2414-1895 DOI: 10.6919/ICJE.202504_11(4).0059

Research Progress of h-BN in Thermal Driven Catalysis

Quanxin Gong*

School of Materials and Chemistry, the University of Shanghai for Science and Technology, Shanghai 200093, China

*Corresponding author Email: usst191410@163.com

Abstract

Hexagonal boron nitride (h-BN), as a novel two-dimensional material, exhibits high thermal conductivity, excellent thermal stability, low thermal expansion coefficient, oxidation resistance, and chemical stability. Its large specific surface area provides abundant active sites and attachment points, offering unique advantages in thermal catalytic reactions. This paper summarizes the main preparation methods of h-BN, including mechanical exfoliation, liquid-phase exfoliation, chemical vapor deposition, and combined physical and chemical methods, analyzing the superiority and characteristics of each preparation method. It investigates the fundamental properties of h-BN and its applications in oxidative dehydrogenation, oxidative desulfurization, and catalytic hydrogenation, explores the mechanisms of h-BN in thermal catalytic reactions, and prospects the future research opportunities and challenges of h-BN.

Keywords

Hexagonal Boron Nitride; Catalyst; Thermal Catalytic Reactions.

1. Introduction

With the continuous advancement of science and technology, renewable energy is gradually replacing part of fossil fuels. However, the development and utilization of renewable energy are still constrained by multiple factors such as cost, environment, geography, and climate, making it impossible to completely replace fossil fuels in industrial production and daily life [1]. Therefore, reducing the emission of pollutants (such as CO_x, SO_x, and NO_x) from waste and optimizing processes such as desulfurization [2] and denitrification [3] have become hot research directions.

In the process of recycling and reusing waste pollutants, catalysts, in an efficient, green, and economical manner, accelerate the conversion of raw materials into high-value-added chemical products and fuels [4]. Two-dimensional (2D) catalyst materials have attracted widespread attention due to their diversity, adjustable structure, and unique electronic properties [5]. Since Professor Andre Geim first discovered graphene, more than twenty 2D materials have emerged [6], including transition metal dichalcogenides (TMDs), metal oxides, layered double hydroxides (LDHs), hexagonal boron nitride (h-BN), graphitic carbon nitride (g-C_3N_4), and metal carbides and nitrides (collectively known as MXenes) [7-9]. The atoms within each layer of 2D materials are bonded by covalent bonds, while adjacent layers are connected by van der Waals forces. The thickness of a single layer is one or a few atomic sizes, allowing it to exist stably independently [10]. Their unique electronic properties have been proven to significantly affect catalytic activity and selectivity, and their large specific surface area provides attachment points for the compounding of other materials [11].

Hexagonal boron nitride (h-BN), as a two-dimensional (2D) material, represents the most stable phase in the boron nitride crystal structure. It has a bandgap of 5.5 to 6.0 eV, exhibits almost no absorption

ISSN: 2414-1895 DOI: 10.6919/ICJE.202504_11(4).0059

of visible light, and appears white, often referred to as "white graphene" [12]. h-BN is sp^2 hybridized, where nitrogen (N) and boron (B) atoms alternately connect to form stable hexagonal rings that extend infinitely in two dimensions, with layers connected by van der Waals forces. h-BN possesses excellent dielectric properties, thermal stability, thermal conductivity, and chemical stability, making it widely applicable in various fields such as adsorption materials, catalytic materials, hydrogen storage materials, thermal insulation materials, dielectric substrates, antioxidants, flame retardants, radiation protection materials, and anti-corrosion materials [13-19]. The functionalization of h-BN can enhance its catalytic performance by introducing defects, element doping, and functional group modifications [20], which create unsaturated B and N vacancies as active catalytic sites. While h-BN has been extensively used in electrocatalysis and photocatalysis, its unique chemical stability still holds significant potential for development in thermal catalysis. For instance, Ji et al. [21] constructed a layer of h-BN and used it as an interlayer confinement carrier for phosphotungstic acid (HPW/h-BN). The resulting HPW/h-BN achieved ~100% desulfurization efficiency in oxidative desulfurization (ODS) and maintained its activity even after six cycles of use.

This article, based on the latest research, analyzes the advantages and characteristics of different synthesis methods for h-BN, and provides a detailed discussion of its applications, reaction mechanisms, and future research directions and challenges in thermal catalytic reactions such as oxidative dehydrogenation, oxidative desulfurization, and hydrogenation. It aims to serve as a reference for researchers in the field of catalysis.

2. The Preparation Methods of h-BN

The synthesis methods of two-dimensional h-BN can be divided into top-down and bottom-up approaches [22]. In nature, h-BN often exists in bulk or multilayer crystal structures with low specific surface areas. The top-down method involves overcoming the van der Waals forces between layers through external shear forces, transforming multilayer structures into few-layer or single-layer structures. The preparation methods of h-BN mainly include mechanical exfoliation and chemical exfoliation. These processes are generally simple, high-yield, and widely applicable, and they can easily create defects within the h-BN plane, which is beneficial for subsequent functionalization [23]. The bottom-up process involves the chemical synthesis of h-BN by adding B and N sources under certain conditions, primarily including chemical vapor deposition (CVD), laser sintering, and thermal decomposition. This approach avoids the agglomeration and stacking of hexagonal boron nitride nanosheets (h-BNNSs), making it easier to obtain high-quality h-BNNSs with controlled morphology and size[24, 25].

2.1 Mechanical Exfoliation

Mechanical exfoliation primarily uses bulk h-BN as the substrate, applying external force (energy) to disrupt the van der Waals forces between h-BN layers. Common methods include ball milling, grinding, ultrasonic exfoliation, and plasma etching, facilitating the transition from multilayer to few-layer structures. Unlike graphene, h-BN's interlayer stronger electronegativity due to elemental differences makes exfoliation more challenging. Zhang et al. [25] employed a straightforward grinding exfoliation method using silicon carbide (SiC) particles as intermediates, applying approximately 100N pressure on a grinder for 270 minutes. The ground 2D h-BN was then separated from the abrasive in deionized water. Atomic force microscopy (AFM) results indicated an average lateral size of 1.2μm for h-BN, with an exfoliation yield as high as 67%. Currently, ball milling is considered the simplest and most effective method for exfoliating h-BN [26]. However, it often results in excessive defects in h-BN crystals and difficulty in obtaining large sizes. Ali et al. [27] introduced low-density polyethylene (LLDPE) during ball milling to reduce crystal defects in h-BN nanosheets (h-BNNSs). From the XRD patterns of LLDPE-milled h-BN (M-hBN), it was observed that with increasing milling time, the (002) diffraction peak of M-hBN broadened and its intensity significantly decreased, indicating exfoliation and the formation of smaller crystallites. The ball-to-material ratio was 10:1, with a milling frequency of 250 rpm and a milling time of 1.5 hours.

ISSN: 2414-1895 DOI: 10.6919/ICJE.202504_11(4).0059

Additionally, the proportion of LLDPE also affected the crystallinity of h-BN. Similar to LLDPE, xylitol ($C_4H_{12}O_5$) as a milling agent not only mitigated defects in h-BN but also inhibited the agglomeration of h-BNNSs.

2.2 Liquid-phase Exfoliation

Liquid-phase exfoliation utilizes small molecules/ions in the liquid phase to penetrate between the layers of h-BN, inducing exfoliation through chemical reactions or phase transitions. Li et al. [28] proposed an improved molten salt-assisted exfoliation (MMSAE) strategy, using LiCl-KCl as the medium. At high temperatures, ions from the liquid medium enter the interlayer space of h-BN, and under magnetic stirring, h-BN nanosheets (h-BNNSs) with an average lateral size of 6.30 μm and a thickness of 2.34 nm were obtained. Since the diameter of H_2O molecules (about 2.75 Å) is smaller than the interlayer spacing of h-BN (around 3.2 Å), aqueous solutions can serve as exfoliation solvents for h-BN. An et al. [29]achieved h-BN exfoliation by utilizing the rapid expansion of water during freezing. The water solution of h-BN was rapidly frozen with liquid nitrogen, and the interlayer water molecules nucleated and expanded quickly. After five freeze-thaw cycles, successful exfoliation of h-BNNSs with a thickness of less than 2 nm was achieved. In addition to water as the solvent, organic solvents such as isopropanol (IPA), N,N-dimethylformamide, N-methylpyrrolidone, and aromatics, which have surface energies similar to that of h-BN, can also act as exfoliation solvents, allowing h-BNNSs to disperse more effectively in the solvent. Chen et al. [30] used a wet chemical method to exfoliate h-BN, employing potassium permanganate and concentrated sulfuric acid as solvents. During the intense reaction, H^+ ions entered the interlayer space of h-BN, while the generated oxygen and ozone produced outward thrust. The resulting edge-hydroxylated h-BNNSs had an average lateral size of 123 nm and a thickness of approximately three layers.

2.3 Chemical Vapor Deposition (CVD)

As a bottom-up synthesis method, Chemical Vapor Deposition (CVD) for preparing h-BN typically uses boron halides, chlorides, or diborane as boron sources [31], and ammonia as the nitrogen source. Transition metals such as Ni, Cu, Pt, Rh, Ru, Pd, and substrates like Al_2O_3 and Si are employed [32, 33]. At high temperatures, the precursors undergo thermal decomposition or chemical reactions on the substrate, resulting in h-BNNSs with controllable thickness and area. The growth conditions, including temperature, duration, reaction sources, gas flow rate, and pressure, significantly influence the growth of h-BN [34-36].

CVD-grown h-BN tends to grow along specific crystallographic directions on the substrate, leading to different morphologies (triangular, hexagonal, or rhombic) on various substrates. Yang et al. [37] used Cu/Ni alloy as a substrate and controlled the growth shape of h-BN by adjusting the Cu/Ni ratio. They found that triangular h-BN domains are more easily formed on pure Cu with a higher nucleation density. With the introduction of Ni, the h-BN domains gradually become more circular, and the nucleation density significantly decreases. When the Ni content reaches 22.7 wt%, the number of h-BN grains grown on the Cu/Ni alloy is ten times less than that on pure Cu foil, making it easier to obtain large single crystals. Additionally, different crystal planes of the same substrate also affect the final growth outcome of h-BN. Zhu et al. [38] systematically investigated the stability of h-BN clusters on Ni(100), Ni(110), and Ni(111) surfaces based on density functional theory (DFT). Compared to the Ni(111) surface, the honeycomb-like h-BN undergoes greater deformation along the z-axis on Ni(100) and Ni(110) surfaces. This difference is primarily attributed to the metal atom packing density, substrate symmetry, deformation of BN clusters, and lattice mismatch between BN clusters and different metal surfaces. Jia et al. [39]directly grew high-quality and uniform h-BN films on stainless steel substrates as anti-corrosion protective layers. With prolonged growth cycles, more h-BN was deposited on the stainless steel surface. When the deposition time reached 5 minutes, the surface coverage approached 100%, although some fine pinholes remained. By extending the deposition time to 15 minutes, these pinholes were completely filled, resulting in a continuous and dense film.

ISSN: 2414-1895 DOI: 10.6919/ICJE.202504_11(4).0059

3. The Application of h-BN in Thermal Catalytic Reactions.

Carbon-based catalytic materials exhibit a broader range of applications than their metal-based counterparts, owing to their resistance to acids and alkalis, as well as their tunable electron density. Nonetheless, in high-temperature, oxygen-rich environments, carbon-based catalysts frequently deactivate due to their limited oxidation resistance [40]. In contrast, h-BN features a robust polar bond between boron (B) and nitrogen (N) atoms. This strong covalent bond endows h-BN with exceptional thermal stability, surpassing that of carbon-based materials. Specifically, h-BN decomposes at 1273 K in air, 1673 K in a vacuum, and up to 3150 K in an inert atmosphere. Moreover, h-BN's remarkable chemical stability ensures its prolonged stability in most acidic solutions and oxidants, thereby minimizing the occurrence of undesirable side reactions [41].

3.1 Oxidative Dehydrogenation Reaction

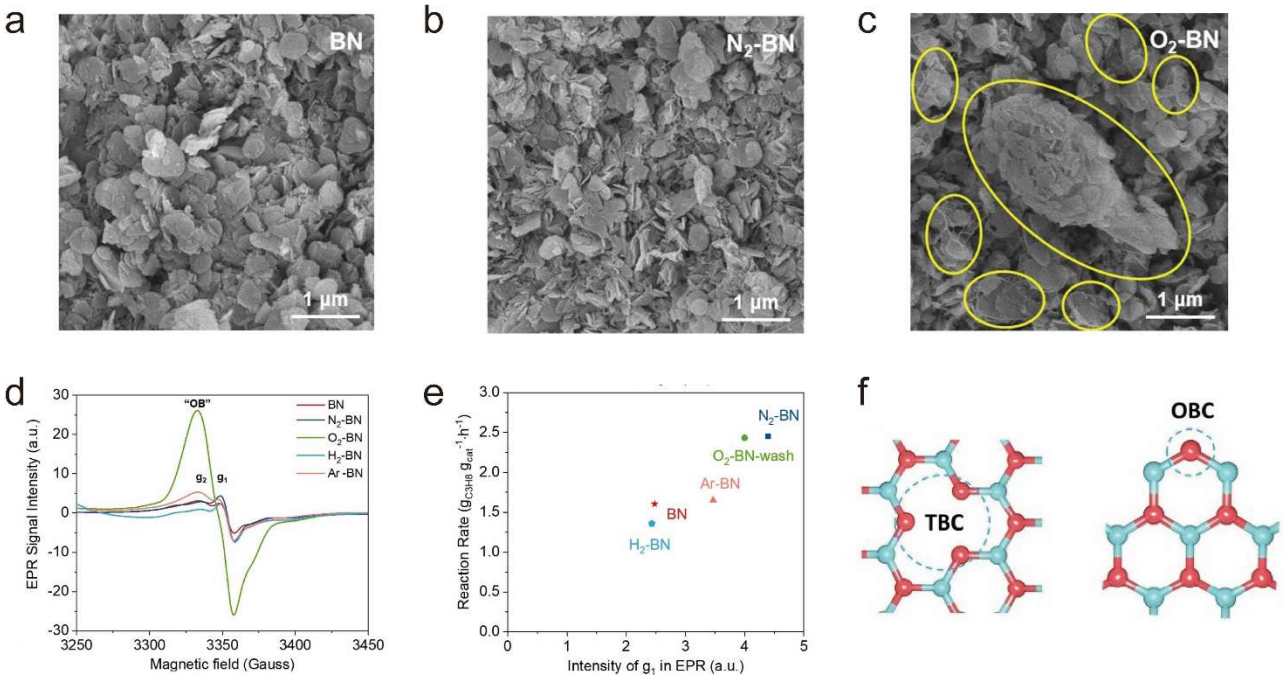

Figure 1. Characterization of h-BN Catalysts in the Oxidative Dehydrogenation Reaction of Light Alkenes. (a, b, c) SEM images of h-BN, N_2-BN, and O_2-BN, respectively. (d) EPR spectrum. (e) Relationship between the unit area reaction rate and the g1 intensity in EPR. (f) TBC and OBC structural models [42].

Hermans et al. [42] employed h-BN as a catalyst in the cracking reaction of propane (C_3H_8), achieving a yield of 79% propylene (C_3H_6) and 12% ethylene (C_2H_4). h-BN demonstrated high selectivity in hydrocarbon catalysis. During the alkane cracking process, h-BN catalysis exhibited an induction period. Zhou et al. [43] treated C_2H_6 and O_2 together and found that a large number of hydroxyl groups (B-OH) were attached to the surface of h-BN. At high temperatures, B-OH combined with O_2 to form B-O groups, which then reacted with C_2H_6 to regenerate B-OH, ultimately achieving the dehydrogenation of C_2H_6 to produce C_2H_4 with an ethylene yield of 110 $\mu molg^{-1}s^{-1}$. The B atoms connected to oxygen were identified as the active sites of h-BN. Rational modification of the catalyst surface is a common method to enhance catalytic activity. Liu et al. [44] treated h-BN with N_2, O_2, H_2, and Ar plasma for the oxidative dehydrogenation (ODH) of C_3H_8. From the SEM images in Figures 1a, 1b, and 1c, it was observed that h-BN treated with O_2 plasma (O_2-BN) aggregated into blocks, while h-BN treated with N_2 plasma (N_2-BN) retained its original morphology. Testing revealed that N_2-BN achieved a propane conversion rate of 26% and a propylene selectivity of 76.7% at 520°C, with an olefin selectivity of 89.4%, significantly higher than h-BN treated with other plasmas. The electron paramagnetic resonance (EPR) spectrum in Figure 1d shows two nitrogen

ISSN: 2414-1895 DOI: 10.6919/ICJE.202504_11(4).0059

defect signals, g1 and g2, corresponding to the tri-boron center (TBC) and the one-boron center (OBC) respectively (Figure 1f). The catalytic rate of h-BN treated with different plasmas is positively correlated with the intensity of g1 (Figure 1e), indicating that the g1 defect plays a major role as an active site in the ODH reaction, a characteristic that has also been theoretically validated. Through extensive model screening, Si et al. [45] identified three active centers: the zigzag edge of boron termination, nitrogen vacancies (tri-boron centers), and O= groups. The process involves two parts: propylene generation and active site regeneration, with energy barriers of 1.20, 0.61, and 0.34 eV respectively. Further dehydrogenation of propylene is a highly endothermic reaction of up to 1.8 eV, which helps prevent deep oxidation of propylene, making the oxidative dehydrogenation of light alkanes highly selective.

3.2 Oxidative Desulfurization Reaction

Sulfur-containing compounds like dibenzothiophene (DBT) and dimethyl benzothiophene (DMBT) in fuel oil not only damage refining equipment and pipelines but also release sulfides (Sox) into the atmosphere, polluting the environment [46]. Currently, fuel desulfurization methods include adsorption desulfurization, extraction desulfurization [47], and oxidative desulfurization (ODS) [48]. Among them, ODS, due to its mild reaction conditions [49], low cost, and outstanding performance, especially with aromatic sulfur compounds [50], has become a new and efficient desulfurization method.

Wu et al. [51] used a simple ball milling method to prepare few-layer h-BN. As shown in the SEM image (Figure 2a), h-BN exhibits an interwoven nanosheet structure with approximately 2-3 layers (Figure 2b). The nitrogen adsorption-desorption isotherm (Figure 2c) reveals a type II hysteresis, indicating that h-BN has a layered structure with a specific surface area of 431 $m^2 g^{-1}$. Using H_2O_2 as the oxidizing agent, the optimal process parameters were determined, with a catalyst loading of 0.06 g, an O/S molar ratio of 5, and a reaction temperature of 80°C, achieving a desulfurization efficiency of 99.4%. After 8 cycles, the catalytic performance showed no significant decline. In the oxidative desulfurization (ODS) process, electron spin resonance (ESR) tests were conducted to investigate the reaction mechanism. When the free radical scavenger (DMPO) was mixed with h-BN, no distinct signal was observed. However, in the presence of H_2O_2, a 1:2:2:1 branching peak was detected, corresponding to the hydroxyl radical (·OH) (Figure 2d). To identify the active catalytic species, radical trapping experiments were conducted (Figure 2e). TBA, $AgNO_2$, and BQ were added to capture hydroxyl radicals (·OH), free electrons (e^-), and superoxide radicals (O_2^-), respectively. The catalytic activity significantly decreased after the introduction of TBA, indicating that ·OH is the active catalytic species. The B atoms at the defects and edges of h-BN promote the generation of ·OH from H_2O_2 (Figure 2f), thus accelerating the ODH reaction.

Doping can disrupt the atomic arrangement in materials, increasing overall entropy and lowering the Gibbs free energy of high-entropy phases . Wei et al. [52] synthesized carbon and oxygen co-doped h-BN (BCNO) catalysts with different atomic orders using ternary deep eutectic solvents (DES) as precursors, introducing the concept of a boundary index to quantify the content of high-entropy structures (HES) in the catalysts. The results showed that the DES with the highest boundary index had the shortest oxidation induction time, with sulfur completely converted within 6 hours. This was attributed to the presence of sufficient active sites in the HES. N-Hydroxyphthalimide (NHPI), an aerobic catalyst, exhibits excellent ODS performance, but its recovery is difficult, and its performance degrades rapidly after multiple uses. To address this issue, Lu et al. [53] established an NHPI/h-BN catalytic system, using azobisisobutyronitrile (AIBN) as a metal-free initiator and oxygen (O_2) as the oxidant. At 120°C, the DBT conversion rate reached 95%, significantly higher than the 55% conversion achieved with NHPI alone. After 7 cycles, the conversion rate remained above 94%, demonstrating that the addition of h-BN effectively enhanced the catalytic activity of NHPI.

ISSN: 2414-1895 DOI: 10.6919/ICJE.202504_11(4).0059

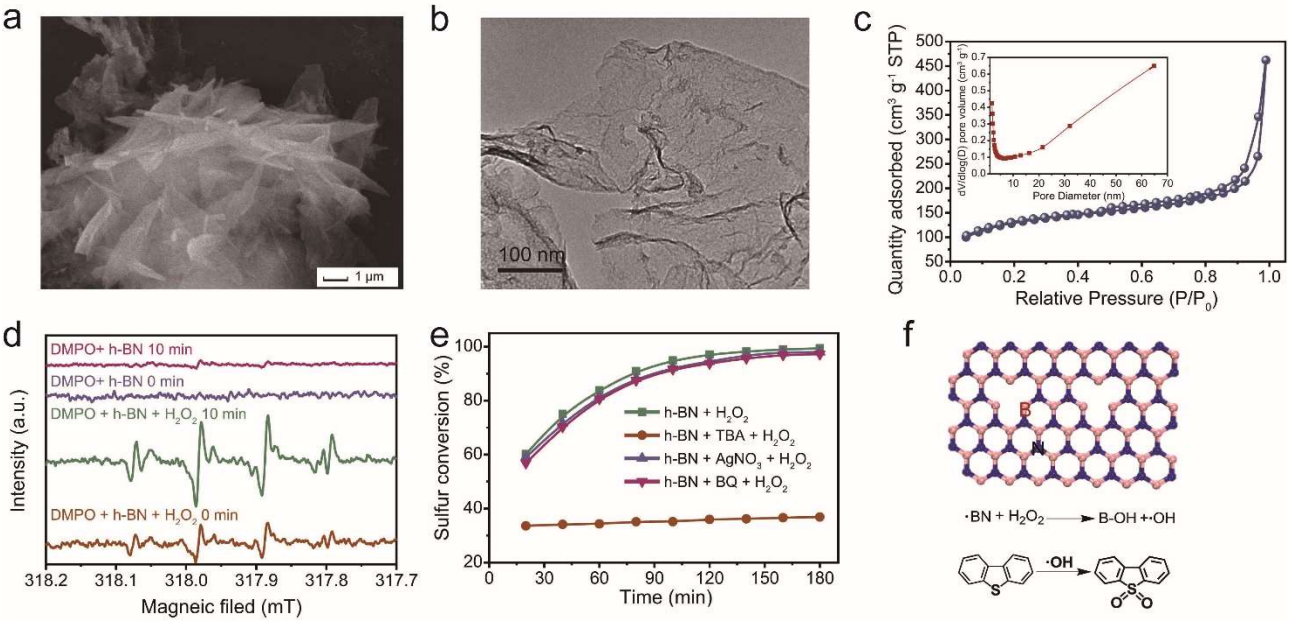

Figure 2. Characterization of catalyst h-BN in oxidative desulfurization reaction. (a) SEM image. (b) TEM image. (c) nitrogen adsorption-desorption curve and corresponding pore size distribution. (d) ESR characterization. (e) radical capture reaction. (f) reaction process diagram [51].

3.3 Hydrogenation Reaction

Selective hydrogenation of unsaturated organic compounds (olefins, alkynes, esters, aldehydes, ketones, imines, etc.) is a crucial process in pharmaceuticals, fine chemicals, and the food industry. Research has shown that the B and N vacancies in hexagonal boron nitride (h-BN) serve as Lewis acid and base centers in catalyzing reactions such as nitro-hydroxy aldehyde transformations and glucose conversion [54].

Cinnamaldehyde (CAL) is a typical α,β-unsaturated aldehyde, as shown in Figure 3a. Upon hydrogenation, CAL can produce the desired cinnamyl alcohol (COL) and the byproduct hydrogenated cinnamaldehyde (HCAL), with excessive hydrogenation leading to the formation of hydrogenated cinnamyl alcohol (HCOL) . Zhang's team [55] developed a porous hexagonal boron nitride (p-BN)-supported cobalt catalyst (Co/p-BN). The preparation involved calcination temperatures of 300 °C, 500 °C, and 800 °C. X-ray diffraction (XRD) patterns revealed the coexistence of h-BN, Co_3O_4, CoO, and Co phases (Figure 3b). As the reduction temperature increased, the cobalt content gradually increased, which helped dissociate H_2 molecules. After a 2-hour evaluation at 140 °C, the Co/p-BN-500 catalyst exhibited the highest CAL conversion rate of 77.4% (Figure 3c), with a COL selectivity approaching 80%. Furthermore, a Pt catalyst supported on h-BN showed superior performance in the selective hydrogenation of cinnamaldehyde, with selectivity above 85% and cinnamaldehyde conversion rates over 95%. This is due to the inert surface and limited acidic and basic sites of the h-BN support, which favor an adsorption mode for reactants that depends on the loaded metal, resulting in high selectivity for cinnamyl alcohol .Huang et al. [56] reported the fixation of oxidized ruthenium (Ru) atoms on defect-rich hexagonal boron nitride (d-BN) nanosheets for the selective hydrogenation of esters. The d-BN, prepared via a one-pot method under high-temperature conditions, exhibited a rich porous structure (Figure 3d), with Ru predominantly existing as single atoms and small nanoclusters (<0.2 nm) distributed on the d-BN surface (Figure 3e). Using the hydrogenation of dimethyl oxalate (DMO) to dimethyl glycolate (MG) as an example, the 1Ru/d-BN catalyst showed a conversion frequency (43.0 h^{-1}) an order of magnitude higher than traditional Ag/SiO_2 catalysts, exhibiting better catalytic selectivity for MG. The DMO conversion rate exceeded 95%, while Ru on the other two inert supports (h-BN and SiO_2) agglomerated into nanoparticles. The DMO conversion rates on 1Ru/h-BN and 1Ru/SiO_2 were 55.4% and 28.9%, respectively, with the generation of methane and other byproducts. This behavior was attributed to

ISSN: 2414-1895 DOI: 10.6919/ICJE.202504_11(4).0059

the dispersed Ru atoms embedded in the defect-rich d-BN, which caused charge transfer from Ru to d-BN, inducing the partial oxidation of $Ru^{\delta+}$ ($3 \leq \delta \leq 4$) active species. The metal-support interactions selectively activated C-O bonds (Figure 8f, blue arrows), whereas Ru nanoclusters supported on defect-free h-BN (Ru/h-BN) exhibited non-selective catalytic hydrogenation of both C-C and C-O bonds (red arrows).

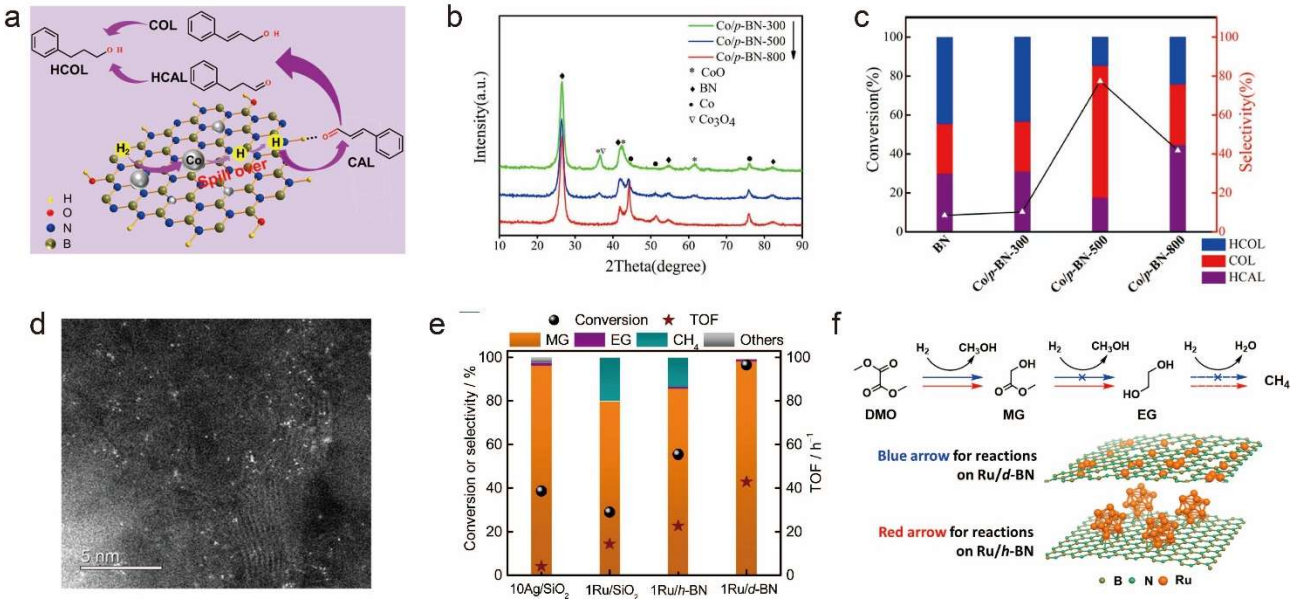

Figure 3. Characterization of h-BN hydrogenation thermocatalytic reaction process. (a) Reaction pathway of cinnamaldehyde hydrogenation. (b) XRD pattern. (c) CAL conversion and selectivity of different products after reaction at 140 °C for 2 h [55]. (d) AC-STEM image of Ru/d-BN. (e) Catalytic performance of different catalysts and TOF. (f) Hydrogenation pathways of Ru/d-BN and Ru/h-BN catalysts (solid arrows and dotted arrows represent one-step irreversible reaction and multi-step irreversible reaction, respectively, and the cross symbol '×' indicates a prohibition reaction) [56].

4. Conclusion and Outlook

In summary, compared to other catalysts, h-BN demonstrates higher selectivity towards products in thermal catalytic reactions. Its unique thermal stability, antioxidant properties, and chemical stability ensure sustained activity under high-temperature conditions. The large specific surface area also facilitates faster reaction rates and improved product conversion. This paper summarizes the main preparation methods for h-BN, provides an in-depth analysis of the thermal catalytic reaction mechanisms of h-BN in oxidative dehydrogenation, oxidative desulfurization, and catalytic hydrogenation reactions, and outlines the latest research progress. Furthermore, it explores the future research opportunities and challenges for h-BN, offering valuable insights for researchers in the catalytic field.

(1)Currently, the main methods for preparing h-BN are mechanical exfoliation, liquid-phase exfoliation, and chemical vapor deposition (CVD), each with its unique advantages but also limitations that need to be addressed. For example, single mechanical exfoliation yields low production rates and it is challenging to obtain monolayer or few-layer h-BN. Combining multiple exfoliation methods effectively can significantly improve exfoliation efficiency. The bottom-up preparation of h-BN requires harsh conditions, and detaching the h-BN from the substrate remains a challenge. Therefore, the development of efficient and controllable methods to produce high-purity few-layer or even monolayer h-BN is essential for future industrial applications.

ISSN: 2414-1895 DOI: 10.6919/ICJE.202504_11(4).0059

(2) h-BN contains abundant defects and edges that serve as active sites and attachment points. Through simple chemical modifications, the in-plane electronic distribution of h-BN can be improved, enhancing its affinity for specific molecules and boosting the intrinsic catalytic activity of h-BN with boron atoms at the center. Additionally, h-BN can act as a support for atomic/nanocluster catalysts, improving catalytic performance while providing a protective shell. However, excessively thick h-BN protective layers may hinder the contact between atomic/nanoclusters and reactants, imposing high demands on the preparation method and material ratios.

(3)With the rapid development of computer technology, multiscale simulation techniques will provide deeper insights into the catalytic mechanisms of h-BN, enabling the design of more precise synthesis strategies. These advancements will gradually address the existing barriers of h-BN and pave the way for its large-scale application.

References

[1] CHEN J, GAO M, SHAHBAZ M, et al. An improved decomposition approach toward energy rebound effects in China: Review since 1992 [J]. Renewable and Sustainable Energy Reviews, 2021.

[2] LI X, HAN J, LIU Y, et al. Summary of research progress on industrial flue gas desulfurization technology [J]. Separation and Purification Technology, 2022.

[3] LEI Z, HAO S, YANG J, et al. Study on denitration and sulfur removal performance of Mn-Ce supported fly ash catalyst [J]. Chemosphere, 2021.

[4] LU Y, ZHANG Z, WANG H, et al. Toward efficient single-atom catalysts for renewable fuels and chemicals production from biomass and CO2 [J]. Applied Catalysis B: Environmental, 2021.

[5] HAN C, ZHANG N, XU Y-J. Structural diversity of graphene materials and their multifarious roles in heterogeneous photocatalysis [J]. Nano Today, 2016.

[6] NOVOSELOV K S. Graphene: materials in the Flatland (Nobel lecture) [J]. Angew Chem Int Ed Engl, 2011.

[7] Zhang H. Ultrathin Two-Dimensional Nanomaterials [J]. Acs Nano, 2015.

[8] XU M, LIANG T, SHI M, et al. Graphene-like two-dimensional materials [J]. Chem Rev, 2013.

[9] BALASUBRAMANIAM B, SINGH N, KAR P, et al. Engineering of transition metal dichalcogenide-based 2D nanomaterials through doping for environmental applications [J]. Molecular Systems Design & Engineering, 2019.

[10] GEIM A K, GRIGORIEVA I V. Van der Waals heterostructures [J]. Nature, 2013.

[11] CHIA X, PUMERA M. Characteristics and performance of two-dimensional materials for electrocatalysis [J]. Nature Catalysis, 2018.

[12] REN J, STAGI L, INNOCENZI P. Hydroxylated boron nitride materials: from structures to functional applications [J]. Journal of Materials Science, 2020.

[13] CHEN H, JIANG D E, YANG Z, et al. Engineering Nanostructured Interfaces of Hexagonal Boron Nitride-Based Materials for Enhanced Catalysis [J]. Acc Chem Res, 2023.

[14] LIANG H, CAO B, ZHU J, et al. Intercalation optimized hexagonal boron nitride nanosheets for high efficiency hydrogen storage [J]. Applied Surface Science, 2022.

[15] JUMA I G, KIM G, JARIWALA D, et al. Direct growth of hexagonal boron nitride on non-metallic substrates and its heterostructures with graphene [J]. iScience, 2021.

[16] REN J, INNOCENZI P. 2D Boron Nitride Heterostructures: Recent Advances and Future Challenges [J]. Small Structures, 2021).

[17] XIONG J, DI J, ZHU W, et al. Hexagonal boron nitride adsorbent: Synthesis, performance tailoring and applications [J]. Journal of Energy Chemistry, 2020.

[18] SUN X, ZHANG J, PAN W, et al. A review on the preparation and application of BN composite coatings [J]. Ceramics International, 2023.

[19] HU P, WANG S, ZHUO Y. Effects of element doping and H2O presence on CO2 adsorption using hexagonal boron nitride [J]. Separation and Purification Technology, 2021.

ISSN: 2414-1895 DOI: 10.6919/ICJE.202504_11(4).0059

[20] QIU M, JIA H, LAN C, et al. An enhanced kinetics and ultra-stable zinc electrode by functionalized boron nitride intermediate layer engineering [J]. Energy Storage Materials, 2022.

[21] YU W, GONG K, LI Y, et al. Flexible 2D Materials beyond Graphene: Synthesis, Properties, and Applications [J]. Small, 2022.

[22] XIONG J, DI J, XIA J, et al. Surface Defect Engineering in 2D Nanomaterials for Photocatalysis [J]. Advanced Functional Materials, 2018.

[23] CUN H, MIAO Z, HEMMI A, et al. High-Quality Hexagonal Boron Nitride from 2D Distillation [J]. ACS Nano, 2021.

[24] BABENKO V, FAN Y, VEIGANG-RADULESCU V-P, et al. Oxidising and carburising catalyst conditioning for the controlled growth and transfer of large crystal monolayer hexagonal boron nitride [J]. 2D Materials, 2020.

[25] ZHANG C, TAN J, PAN Y, et al. Mass production of 2D materials by intermediate-assisted grinding exfoliation [J]. National Science Review, 2020.

[26] DING J-H, ZHAO H-R, YU H-B. High-yield synthesis of extremely high concentrated and few-layered boron nitride nanosheet dispersions [J]. 2D Materials, 2018.

[27] ALI M, ABDALA A. Large scale synthesis of hexagonal boron nitride nanosheets and their use in thermally conductive polyethylene nanocomposites [J]. International Journal of Energy Research, 2021.

[28] LI Z, LI K, LI Y, et al. Modified Molten Salt Assisted Exfoliation of Large-Size 2D Materials [J]. Advanced Functional Materials, 2023.

[29] AN L, GU R, ZHONG B, et al. Water-icing-triggered scalable and controllable exfoliation of hexagonal boron nitride nanosheets [J]. Cell Reports Physical Science, 2022.

[30] CHEN C, SHAO C, WANG A. Chemical exfoliating of boron nitride into edge-hydroxylated nanosheets [J]. Journal of Materials Science, 2023.

[31] ZHANG J, TAN B, ZHANG X, et al. Atomically Thin Hexagonal Boron Nitride and Its Heterostructures [J]. Adv Mater, 2021.

[32] CHEN V, SHIN Y C, MIKHEEV E, et al. Application-driven synthesis and characterization of hexagonal boron nitride deposited on metals and carbon nanotubes [J]. 2D Materials, 2021.

[33] OH H, YI G C. Synthesis of Atomically Thin h-BN Layers Using BCl(3) and NH(3) by Sequential-Pulsed Chemical Vapor Deposition on Cu Foil [J]. Nanomaterials (Basel), 2021.

[34] RUCKHOFER A, SACCHI M, PAYNE A, et al. Evolution of ordered nanoporous phases during h-BN growth: controlling the route from gas-phase precursor to 2D material by in situ monitoring [J]. Nanoscale Horiz, 2022.

[35] WEI W, PAN J, EUARUKSAKUL C, et al. Dynamic observation of in-plane h-BN/graphene heterostructures growth on Ni(111) [J]. Nano Research, 2020.

[36] OKIGAWA Y, MASUZAWA T, WATANABE K, et al. Temperature dependence of carrier mobility in chemical vapor deposited graphene on high-pressure, high-temperature hexagonal boron nitride [J]. Applied Surface Science, 2021.

[37] YANG H, WANG L, GAO F, et al. Shape evolution of two dimensional hexagonal boron nitride single domains on Cu/Ni alloy and its applications in ultraviolet detection [J]. Nanotechnology, 2019.

[38] ZHU H, ZHAO R. Nucleation of CVD-prepared hexagonal boron nitride on Ni(100), Ni(110) and Ni(111) surfaces: A theoretical study [J]. Vacuum, 2022.

[39] JIA S, CHEN W, ZHANG J, et al. CVD growth of high-quality and large-area continuous h-BN thin films directly on stainless-steel as protective coatings [J]. Materials Today Nano, 2021.

[40] WANG L, WANG Y, ZHANG R, et al. Edge-Activating CO2-Mediated Ethylbenzene Dehydrogenation by a Hierarchical Porous BN Catalyst [J]. ACS Catalysis, 2020.

[41] RAFIQ M, HU X, YE Z, et al. Recent advances in structural engineering of 2D hexagonal boron nitride electrocatalysts [J]. Nano Energy, 2022.

[42] Grant J T, Carrero C A, Goeltl F, et al. Selective oxidative dehydrogenation of propane to propene using boron nitride catalysts [J]. Science, 2016.

[43] ZHOU Y, LIN J, LI L, et al. Enhanced performance of boron nitride catalysts with induction period for the oxidative dehydrogenation of ethane to ethylene [J]. Journal of Catalysis, 2018.

ISSN: 2414-1895 DOI: 10.6919/ICJE.202504_11(4).0059

[44] LIU Z, YAN B, MENG S, et al. Plasma Tuning Local Environment of Hexagonal Boron Nitride for Oxidative Dehydrogenation of Propane [J]. Angewandte Chemie International Edition, 2021.

[45] SI C, LIAN Z, OLANRELE S O, et al. Revealing the origin of the reactivity of metal-free boron nitride catalysts in oxidative dehydrogenation of propane [J]. Applied Surface Science, 2020.

[46] CHANDRA SRIVASTAVA V. An evaluation of desulfurization technologies for sulfur removal from liquid fuels [J]. RSC Adv, 2012.

[47] XIONG J, LUO J, DI J, et al. Macroscopic 3D boron nitride monolith for efficient adsorptive desulfurization [J]. Fuel, 2020.

[48] LI C, ZHANG J, LI Z, et al. Extraction desulfurization of fuels with 'metal ions' based deep eutectic solvents (MDESs) [J]. Green Chemistry, 2016.

[49] YANG H, ZHANG Q, ZHANG J, et al. Cellulose nanocrystal shelled with poly(ionic liquid)/polyoxometalate hybrid as efficient catalyst for aerobic oxidative desulfurization [J]. J Colloid Interface Sci, 2019.

[50] ZHANG H, ZHANG Q, ZHANG L, et al. Acidic polymeric ionic liquids based reduced graphene oxide: An efficient and rewriteable catalyst for oxidative desulfurization [J]. Chemical Engineering Journal, 2018.

[51] WU P, LU L, HE J, et al. Hexagonal boron nitride: A metal-free catalyst for deep oxidative desulfurization of fuel oils [J]. Green Energy & Environment, 2020.

[52] WEI Y, ZHANG M, WU P, et al. Deep eutectic solvent-induced high-entropy structures in boron nitride for boosted initiation of aerobic oxidative desulfurization of diesel [J]. Applied Surface Science, 2020.

[53] LU L-J, WU P-W, HE J, et al. N-hydroxyphthalimide anchored on hexagonal boron nitride as a metal-free heterogeneous catalyst for deep oxidative desulfurization [J]. Petroleum Science, 2022.

[54] NAMBA S, TAKAGAKI A, JIMURA K, et al. Effects of ball-milling treatment on physicochemical properties and solid base activity of hexagonal boron nitrides [J]. Catalysis Science & Technology, 2019.

[55] ZHANG R, WANG L, YANG X, et al. The role of surface N H groups on the selective hydrogenation of cinnamaldehyde over Co/BN catalysts [J]. Applied Surface Science, 2019.

[56] HUANG L, LIU X-F, ZOU J, et al. Atomic ruthenium stabilized on vacancy-rich boron nitride for selective hydrogenation of esters [J]. Journal of Catalysis, 2022.